

Characterizing Noise of Driven Controlled Field Using the Central Spin Model

R. Jafari,^{1, 2, 3,*} A. Asadian,¹ M. Abdi,⁴ and Alireza Akbari^{5, 6}

¹*Department of Physics, Institute for Advanced Studies in Basic Sciences (IASBS), Zanjan 45137-66731, Iran*

²*School of Nano Science, Institute for Research in Fundamental Sciences (IPM), 19395-5531, Tehran, Iran*

³*Department of Physics, University of Gothenburg, SE 412 96 Gothenburg, Sweden*

⁴*Wilczek Quantum Center, School of Physics and Astronomy,
Shanghai Jiao Tong University, Shanghai 200240, China*

⁵*Beijing Institute of Mathematical Sciences and Applications (BIMSA), Huairou District, Beijing 101408, P. R. China*

⁶*Institut für Theoretische Physik III, Ruhr-Universität Bochum, 44801 Bochum, Germany*

(Dated: September 4, 2024)

We analyze the coherence dynamics of a central spin coupled to a spin chain with a time-dependent noisy magnetic field, focusing on how noise influences the system's decoherence. Our results show that decoherency due to the nonequilibrium critical dynamics of the environment is amplified in the presence of uncorrelated and correlated Gaussian noise. We demonstrate that decoherence factor consistently signals the critical points, and exhibits exponential scaling with the system size, the square of noise intensity, and the noise correlation time at the critical points. We find that strong coupling between the qubit and the environment allows partial revivals of coherence, which diminish with increasing noise intensity or decreasing noise correlation time. In contrast, weak coupling leads to monotonic enhanced decoherence. The numerical results illustrate that, the revivals decay and scale exponentially with noise intensity. Moreover, the revivals increase and indicate linear or power law scaling with noise correlation time depends on how the correlated noise is fast or slow. Additionally, we explore the non-Markovianity of the dynamics, finding that it decays in the presence of noise but increases as the noise correlation time grows. Our findings have potential applications in the noise spectroscopy of external signals.

I. INTRODUCTION

Quantum correlations (QCs) play a fundamental role in quantum information science [1, 2] and quantum computation [3–6], as they are crucial for understanding the non-locality inherent in quantum mechanics [7, 8]. In quantum information processing, quantum systems are unavoidably influenced by interactions with their surrounding environment. These interactions lead to quantum decoherence, which is essential for comprehending the transition from quantum to classical behavior [9–13]. To explore the decoherence of a qubit caused by its interaction with an environment (spin bath) near a quantum critical point (QCP) [14], a well-established model, the central spin model (CSM) [15–20], has been extended to the context of quantum phase transitions [11, 21]. In the CSM, a central spin (CS) or qubit is globally coupled to an environmental quantum spin system (ESS), which may be either time-independent or time-dependent.

In the time-independent case, the environmental spin system is initially prepared in its ground state, while the central spin/qubit is in a pure state. The global coupling between the qubit and the environment is designed such that the subsequent time evolution of the ESS's initial ground state wave function follows two distinct channels, each governed by a different Hamiltonian. Despite the qubit being initially in a pure state, it has been demonstrated that it loses nearly all of its purity when the ESS approaches its quantum critical point [11, 21].

Moreover, in the time-dependent case, when the ESS is slowly driven across its quantum critical point, decoherence is significantly amplified. This enhancement is not only due to the increased susceptibility near the critical point but also due to the provoked excitations, indicating a universality-class-dependent behavior. This behavior shows a striking resemblance to the dynamics of defect formation observed in nonequilibrium phase transitions (Kibble-Zurek mechanism) [22, 23].

However, relatively little attention has been given to the study of stochastically driven ESSs with noisy Hamiltonians, and the role of quantum coherence in such systems remains largely unexplored. In any real experiment, the simulation of the desired time-dependent Hamiltonian is inherently imperfect, and noisy fluctuations are unavoidable. In other words, noise is ubiquitous and inescapable in any physical system, such as noise-induced heating, which can arise from amplitude fluctuations of the lasers forming the optical lattice [24–27]. Consequently, understanding the impact of noise on Hamiltonian evolution is crucial for accurately predicting experimental outcomes and designing sophisticated setups that are robust against noise effects [24, 28–33].

The question addressed in this paper is: What are the effects of a noisy ESS on the decoherence of a central qubit when it is driven across the QCPs? Specifically, is there still a universal pattern in the dynamically induced decoherence, as measured by the decoherence factor (DF) of the CS?

We demonstrate that decoherence factor decreases in the presence of both correlated (colored) and uncorrelated (white) Gaussian noises. This reduction exhibits

* jafari@iasbs.ac.ir, raadmehr.jafari@gmail.com

exponential scaling with the system size, the square of noise intensity, and the noise correlation time at the critical points. Moreover, in the case of strong environment-qubit coupling (large ramp time scale), decoherence exhibits revivals in both noiseless and noisy scenarios. These revivals scale exponentially with the square of noise intensity. However, in the presence of fast colored noise (small correlation time), the revivals scale linearly with the noise correlation time, whereas in slow noise (large correlation time), they exhibit a power-law scaling with noise correlation time. Additionally, we find that the measure of non-Markovianity decreases with the square of noise intensity and increases linearly with the noise correlation time.

II. THEORETICAL MODEL

We consider the decoherence of a qubit coupled to a driven Ising chain that undergoes a quantum phase transition, as illustrated in Fig. 1. The total Hamiltonian of the system is expressed as

$$\mathcal{H} = \mathcal{H}_E + \mathcal{H}_I + \mathcal{H}_q, \quad (1)$$

where

$$\mathcal{H}_E = \mathcal{H}_E(h(t)) = - \sum_{j=1}^N \left(J \sigma_j^x \sigma_{j+1}^x + h(t) \sigma_j^z \right),$$

represents the transverse field Ising model in a ring configuration,

$$\mathcal{H}_I = \mathcal{H}_I(\delta) = -\delta \sum_{j=1}^N \sigma_j^z \sigma_0^z,$$

describes the interaction between the central qubit and the surrounding spin ring, and

$$\mathcal{H}_q = \sigma_0^z,$$

corresponds to the Hamiltonian of the qubit. Here, $\sigma^{\alpha=x,y,z}$ are Pauli matrices, and δ represents the interaction strength between the qubit and the ring (environment). We consider the parameter $h(t) = h_0(t) + R(t)$, in which $h_0(t)$ to be quenched from an initial value h_i at time t_i following the linear quench protocol $h_0(t) = t/\tau_Q$, to a final value $h_0(t)$ at time t , where τ_Q is the ramp time scale, and $R(t)$ is the stochastic noise. When the field is time-independent and noiseless, $h_0(t) = h$, the ground state is ferromagnetic for $|h| < 1$, otherwise paramagnetic, with the phases separated by equilibrium quantum critical points at $h_c = \pm 1$ [34].

Assuming the qubit is initially in a pure state,

$$|\phi(-\infty)\rangle_q = |\phi(t_i = -\infty)\rangle_q = c_u |\uparrow\rangle + c_d |\downarrow\rangle,$$

with coefficients satisfying $|c_u|^2 + |c_d|^2 = 1$, and the environment, E , is in the ground state denoted by

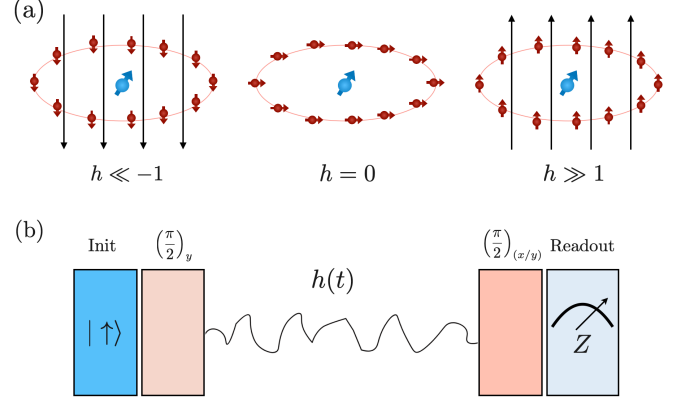


FIG. 1. (a) The central spin-1/2 qubit interacts with an Ising spin environment, where a quantum phase transition is induced by an external magnetic field. When the initial and final fields are large ($|h(t)| > 1$), as shown in the right and left panels, respectively, the environment is in a paramagnetic phase, with its spins aligning with the field. In contrast, when the field is small ($|h(t)| < 1$; center panel), the Ising chain enters a ferromagnetic phase, where its spins attempt to align along the x or $-x$ direction, thereby breaking the symmetry of the Ising Hamiltonian. (b) The decoherence factor can be directly measured through a Ramsey experiment, which involves a $\pi/2$ pulse sequence followed by a projective measurement in the Z -basis on the central qubit.

$|\varphi(-\infty)\rangle_E = |\varphi(t_i = -\infty)\rangle_E$, the total wave function of the composite system at time $t_i = -\infty$ can then be written in the direct product form

$$|\Psi(t_i = -\infty)\rangle = |\phi(-\infty)\rangle_q \otimes |\varphi(-\infty)\rangle_E. \quad (2)$$

A straightforward calculation shows that the total wave function at an instant t is given by [35]

$$|\Psi(t)\rangle = c_d |\downarrow\rangle \otimes |\varphi_-(t)\rangle + c_u |\uparrow\rangle \otimes |\varphi_+(t)\rangle, \quad (3)$$

where

$$|\varphi_{\pm}(t)\rangle = \hat{T} \exp \left[-i \int_{t_i}^t \mathcal{H}_E(h(t) \pm \delta) dt \right] |\varphi(t_i)\rangle, \quad (4)$$

and \hat{T} denotes the time-ordering operator. Since interaction Hamiltonian commutes with the central spin Hamiltonian, the basis $\{|\uparrow\rangle, |\downarrow\rangle\}$ are stationary states. Thus, the evolution of the entire system simplifies to the dynamics of two Ising branches, each evolving in an effective magnetic field given by $h_{\text{eff}}(t) = h(t) \pm \delta$. Consequently, the spin-dependent evolution of the environmental states is governed by

$$i \frac{\partial}{\partial t} |\varphi_{\pm}(t)\rangle = \mathcal{H}_E(h(t) \pm \delta) |\varphi_{\pm}(t)\rangle. \quad (5)$$

Given the qubit in the $|\uparrow\rangle, |\downarrow\rangle$ basis, the reduced density matrix is described by [35]

$$\rho_S(t) = \text{Tr}_E [|\psi(t)\rangle \langle \psi(t)|] = \begin{pmatrix} |c_u|^2 & c_u c_d^* d^*(t) \\ c_u^* c_d d(t) & |c_d|^2 \end{pmatrix}, \quad (6)$$

where $d(t) = \langle \varphi_+(t) | \varphi_-(t) \rangle$ captures the coherency of the spin. We focus on studying its squared modulus, $|d(t)|^2$, which is known as the decoherence factor, to analyze the time evolution of coherence:

$$D = |d(t)|^2 = |\langle \varphi_+(t) | \varphi_-(t) \rangle|^2. \quad (7)$$

Not to be confused with the term noise, it is preferable to refer to this property as visibility, which measures the interference contrast. It is worth noting that the entanglement entropy, concurrence, and maximum quantum Fisher information are directly connected to the decoherence factor [36–38]. The qubit is fully decohered when $D = 0$, but it stays in a pure superposition state when $D = 1$. In the unique situation where $c_u = c_d = 1/\sqrt{2}$, the density matrix assumes the subsequent straightforward form

$$\rho_S(t) = \frac{1}{2} \begin{pmatrix} 1 & d^*(t) \\ d(t) & 1 \end{pmatrix} = \frac{1}{2} \left(\mathbb{1} + \langle \sigma_0^x \rangle \sigma_0^x + \langle \sigma_0^y \rangle \sigma_0^y \right). \quad (8)$$

From this, it becomes evident that one can directly measure D by evaluating the Pauli x and y observables of the central spin. Specifically, $d(t) = \langle \sigma_0^x \rangle + i \langle \sigma_0^y \rangle$. The standard experimental scheme to perform this measurement is known as the Ramsey measurement, which involves suitable pulse sequences followed by a projective measurement in the Z -basis, as illustrated in Fig. 1(b). In this scheme, the first pulse performs a $\pi/2$ -rotation of the initial qubit state around the y -axis. The second pulse applies another $\pi/2$ -rotation, but around either the x -axis or the y -axis, depending on whether σ_0^x or σ_0^y is to be measured. The outcome statistics are then read out in the Z -basis to determine the expectation values of σ_0^y or σ_0^x .

A. Decoherence factor and time dependent Schrödinger equation

The dynamics of the decoherence factor (visibility) can be obtained by solving the time dependent Schrödinger equation (Eq. 5). By performing the Jordan-Wigner fermionization and utilizing the Fourier transformation [39, 40], the Hamiltonian of Eq. (1) can be expressed as the sum of $N/2$ non-interacting terms:

$$H(t) = \sum_k \mathcal{H}_k(t), \quad (9)$$

with

$$\mathcal{H}_k(t) = [(h(t) \pm \delta - \cos k)](c_k^\dagger c_k + c_{-k}^\dagger c_{-k}) + \sin(k)(c_k^\dagger c_{-k}^\dagger + c_k c_{-k}), \quad (10)$$

where c_k (c_k^\dagger) represents spinless fermionic annihilation (creation) operator, and the wave number k is given by $k = (2m-1)\pi/N$, with m ranging from 1 to $N/2$, and N denotes the total number of spins (or sites) in the chain. The above equations indicate that the Hamiltonian of N

interacting spins, as given in Eq. (1), can be transformed into the sum of $N/2$ non-interacting quasi-spins. The Bloch single-particle Hamiltonian $\mathcal{H}_k(t)$ can be expressed as

$$\mathcal{H}_k(t) = \begin{pmatrix} h_z(k, t) & h_{xy}(k) \\ h_{xy}(k) & -h_z(k, t) \end{pmatrix}, \quad (11)$$

where $h_{xy}(k) = \gamma \sin(k)$ and $h_z(k, t) = h(t) - J \cos(k)$. Thus, the time-dependent Schrödinger equation (Eq. (5)) can be expressed as

$$\begin{aligned} i \frac{d}{dt} v_k^\pm &= -(h(t) \pm \delta - \cos k) v_k^\pm + \sin k u_k^\pm, \\ i \frac{d}{dt} u_k^\pm &= (h(t) \pm \delta - \cos k) u_k^\pm + \sin k v_k^\pm. \end{aligned} \quad (12)$$

Within this framework, one can derive that

$$D(t) = \prod_{k>0} F_k(t); \quad F_k(t) = |u_k^{+*}(t)u_k^-(t) + v_k^{+*}(t)v_k^-(t)|^2, \quad (13)$$

where $F_k(t)$ captures the dynamics of decoherence from the perspective of momentum space [41].

It is worthy to note that, in the absence of noise $R(t) = 0$, it can be demonstrated that the coupled differential equations in Eq. (12) are exactly solvable [35, 41–44]. While in the presence of noise, the ensemble average of $u_k^\pm(t)$ and $v_k^\pm(t)$ can be calculated numerically using the master equation [42–46]. In the following we first review the dynamics of decoherence factor in the noiseless case and then we search the effects of noise on the dynamics of decoherence factor.

III. NOISELESS DECOHERENCE FACTOR

The quench begins with the environment in the paramagnetic phase ($h_0(t) < -1$), transitions it through the ferromagnetic phase ($-1 < h_0(t) < 1$), and finally brings it to the other paramagnetic phase ($h_0(t) > 1$), where the critical points are located at $h_c = \pm 1$. As the field polarizing spins in the chain is ramped up, the environment's sensitivity to external influences grows. This heightened sensitivity leads to enhanced decoherence, which is observed as a gradual reduction in the decoherence factor D away from the critical point; see Fig. 2. In the noiseless case, it has been shown that the decoherence factor in the paramagnetic phase is approximately given by [35]

$$D(t) \approx \exp \left(-\frac{N\delta^2}{4h(t)^2(h(t)^2 - 1)} \right). \quad (14)$$

Just above the first critical point, $h > -1$, the adiabatic approximation breaks down and decoherence speeds up; decoherence factor decreases substantially. This happens because (i) the environment's sensitivity is enhanced by quantum criticality, which amplifies the perturbation due

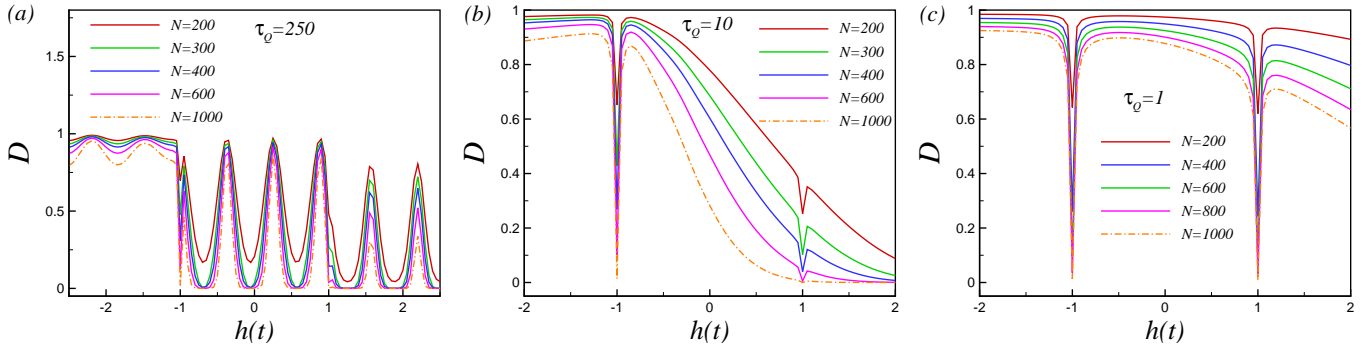


FIG. 2. Noiseless decoherence, as measured by the visibility or decoherence function during a quench, is analyzed for $\delta = 0.01$ with varying ramp time scales τ_Q and system sizes N : (a) For $\tau_Q = 250$, a quasi-periodic regime is observed between the critical points. In this regime, nearly perfect revivals of coherence occur between the critical points. However, coherence is almost completely lost after the environment is driven through the second critical point, especially for large system sizes $N \geq 1000$. (b) For $\tau_Q = 10$, there is a monotonic decay of coherence between the critical points. This behavior is observed when τ_Q exceeds the threshold value of $\pi/(16\delta)$, indicating that τ_Q is approximately around this threshold. (c) The decoherence behavior during the quench for $\tau_Q = 1$ is illustrated, highlighting the differences in coherence loss compared to the other time scales.

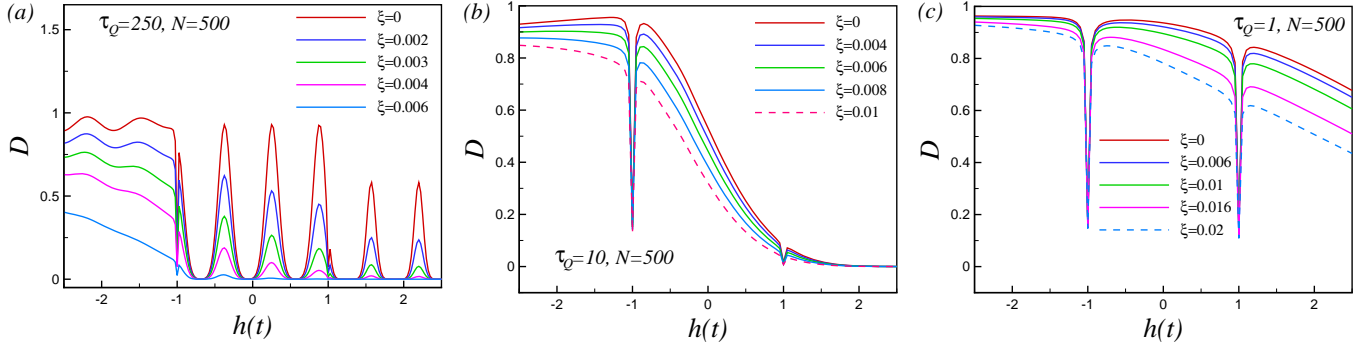


FIG. 3. The noisy decoherence during a quench in the presence of the white noise, for $\delta = 0.01$, $N = 500$ and different values of τ_Q and noise intensity: (a) As seen, revivals of coherence which take place between the critical points for the ramp time scale $\tau_Q = 250$, are still partially present in the presence of the white noise. (b) Monotonic decay of coherence between the critical points for $\tau_Q = 10$ increases in the presence of the white noise. (c) Illustrates decay of the noisy decoherence during the quench for $\tau_Q = 1$.

to the coupling with the qubit system; and (ii) the environment is no longer in its ground state, as the quench is taking it into a superposition of energy eigenstates [42–44, 47]. As the environment is driven past the first critical point at $h_c = -1$, coherence either partially revives [Fig. 2(a)] or decays monotonically [Figs. 2(b) and 2(c)] in the region between the critical points. These behaviors arise from the non-equilibrium dynamics near the critical point, where small k modes are excited as the gap in the excitation spectrum closes for $k = \pi$ at $h_c = -1$. The low k modes, particularly those with $k \sim \hat{k} \sim \tau_Q^{-1/2}$ [35], experience significant excitation, while the larger k modes, for which $k \gg \hat{k}$, evolve adiabatically through the critical point. Additionally, partial revivals of coherence between the critical points have been observed when the environment-qubit coupling is sufficiently strong, specifically when $\delta \gg \pi/(16\tau_Q)$ [35]; see Fig. 2(a). These revivals manifest within the magnetic field, $h(t)$, domain with a period of $\pi/(4\tau_Q\delta)$ [35]. In contrast, in the weak coupling regime where $\delta \ll \pi/(16\tau_Q)$, the decoherence

factor exhibits a monotonic decrease, as illustrated in Fig. 2(b). Moreover, more complex decoherence dynamics arise when the magnetic field reverses polarity and drives the system past the second critical point at $h_c = 1$. At this second critical point, modes with $k \sim \pi - \hat{k}$ become excited due to the gap closing at $k = \pi$.

In the next section we will study the effect of noise on the dynamics of the decoherence factor using the numerical solution of the exact master equation.

IV. IMPACT OF ENVIRONMENTAL NOISE: NOISY DYNAMICS

Noise is everywhere and unavoidable in any physical system. Specifically, when energy is moved into or out of a system in the lab, there will always be some fluctuations, “noise”, in this process. In addition, in the Ramsey interference scheme, we use the central qubit as a noise spectrometer. The noise is caused by a classical fluctu-

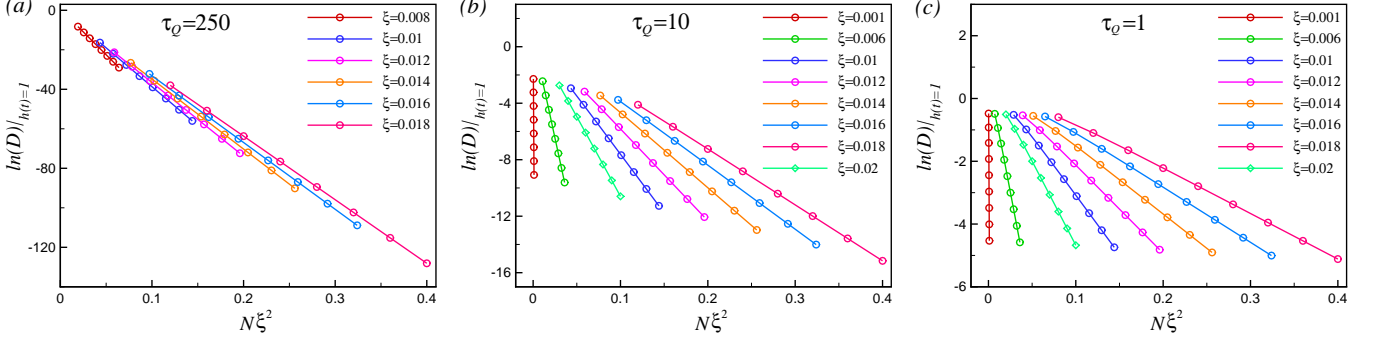


FIG. 4. Scaling of the minimum decoherence at the critical point $h_c = 1$ versus $N\xi^2$ for the different ramp time scales: (a) $\tau_Q = 250$, (b) $\tau_Q = 10$, (c) $\tau_Q = 1$.

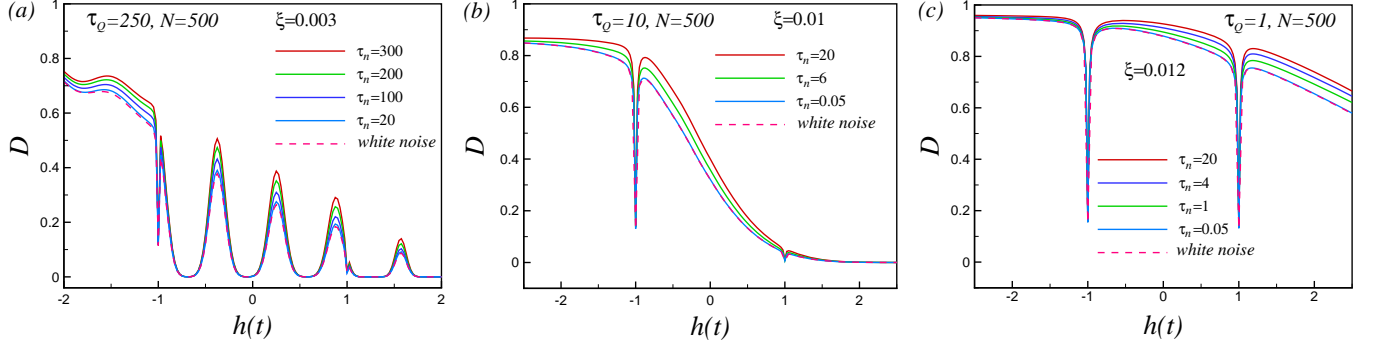


FIG. 5. The noisy decoherence during a quench in the presence of colored noise, with parameters $\delta = 0.01$ and $N = 500$: (a) For $\tau_Q = 250$ and $\xi = 0.003$, revivals of coherence observed between critical points in the ramp time scale $\tau_Q = 250$ are also partially visible in the presence of colored noise. (b) For $\tau_Q = 10$ and $\xi = 0.01$, there is a monotonic decay of coherence between critical points, which becomes more pronounced with an increase in τ_n . (c) For $\tau_Q = 1$ and $\xi = 0.012$, the decay of noisy decoherence is shown for a quench with $\tau_Q = 1$.

ating field. In this section, we look at how noise affects the decoherence of a qubit that's linked to a time-varying environmental spin system. To this end, we consider an added noise to the time dependent magnetic field

$$h(t) = h_0(t) + R(t) = \frac{t}{\tau_Q} + R(t), \quad (15)$$

where $R(t)$ represents random fluctuations confined to the ramp interval $[t_i = h_i \tau_Q, t_f = h(t) \tau_Q]$, with vanishing mean, $\langle R(t) \rangle = 0$. We use colored noise (Ornstein-Uhlenbeck process) with Gaussian two-point correlations

$$\langle R(t)R(t') \rangle = \frac{\xi^2}{2\tau_n} e^{-\frac{|t-t'|}{\tau_n}},$$

where ξ characterizes the strength of the noise and τ_n is the noise correlation time [42, 46, 48–50]. White noise is approximately equivalent to fast colored noise ($\tau_n \rightarrow 0$) with two-point correlations

$$\langle R(t)R(t') \rangle = \xi^2 \delta(t - t').$$

In the presence of noise, the transition probability is obtained by numerically solving the exact master equation [42, 46, 48–50] for the averaged density matrix $\rho_k(t)$

of the noisy Hamiltonian

$$H_k^{(\xi)}(t) = H_k^{(0)}(t) + R(t)H_k^{(1)}, \quad (16)$$

i.e.,

$$\begin{aligned} \dot{\rho}_k(t) = & -i[H_k^{(0)}(t), \rho_k(t)] \\ & - \frac{\xi^2}{2\tau_n} \left[H_k^{(1)}, \int_{t_i}^t e^{-|t-s|/\tau_n} [H_k^{(1)}, \rho_k(s)] ds \right]. \end{aligned} \quad (17)$$

where $H_k^{(0)}(t)$ represents the noise-free Hamiltonian and $H_k^{(1)} = -\sigma^z$ denotes the noisy component [42].

As described in Appendix A, by converting Eq. (17) into a pair of coupled differential equations, we numerically compute the mean values of $|u_k^\pm(t)|^2$, $|v_k^\pm(t)|^2$, $u_k^\pm(t)v_k^{\pm*}(t)$, and $u_k^{\pm*}(t)v_k^\pm(t)$ as ensemble averages over the noise distribution $R(t)$. It is important to note that in the limit as $\tau_n \rightarrow 0$, the above master equation simplifies to the white noise master equation

$$\dot{\rho}_k(t) = -i[H_k^{(0)}(t), \rho_k(t)] - \frac{\xi^2}{2} \left[H_k^{(1)}, [H_k^{(1)}, \rho_k(t)] \right]. \quad (18)$$

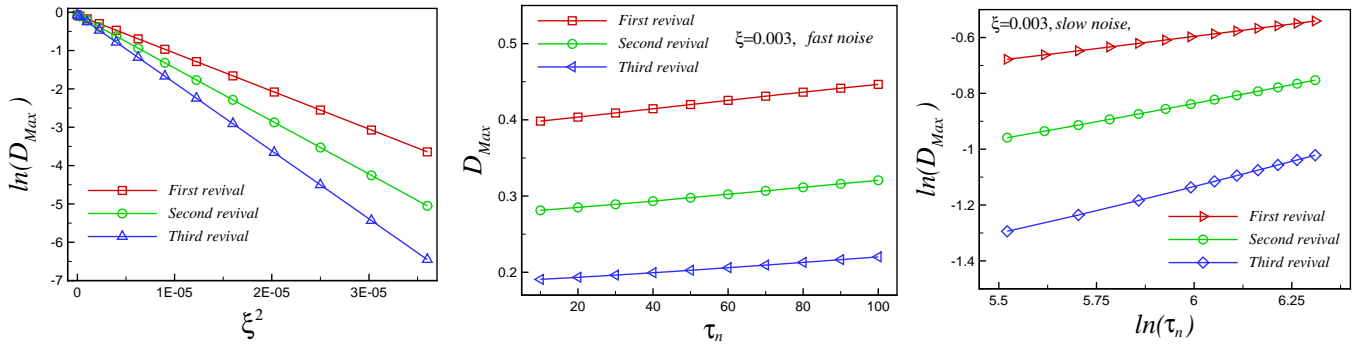


FIG. 6. Scaling of the maximums (revivals) of decoherence (D_{Max}) at the presence of the white noise and colored noise for $\tau_Q = 250$. (a) Linear scaling of $\ln(D_{Max})$ with square of noise intensity ξ^2 corresponding to Fig. 3(a). (b) Linear scaling of revivals (D_{Max}) for noise intensity $\xi = 0.003$ with noise correlation τ_n for fast noise corresponding to Fig. 5(a). (c) Scaling of $\ln(D_{Max})$ versus $\ln(\tau_n)$ for slow noise corresponding to Fig. 5(a) for noise intensity $\xi = 0.003$.

A. Analysis in the presence of white noise

Our numerical analysis begins by examining the effects of white noise on the system, as illustrated in Fig. 3 for ramp time scales: (a) $\tau_Q = 250$, (b) $\tau_Q = 10$, and (c) $\tau_Q = 1$. As depicted in Fig. 3(a), when the environment-qubit coupling is strong, partial revivals are still observable in the presence of the white noise, and diminish by increasing the noise intensity ξ . While, in the absence of noise, the revivals do not decrease by increasing the quench time t , the partial revivals decay by increasing the quench time in the presence of the noise. Decaying the revivals by increasing the quench time in the presence of the noise originates from the accumulation of noise-induced excitations during the evolution. Notably, the period of the revivals remains consistent across both noisy and noiseless cases. In scenarios with weak coupling between the environment and the qubit, as shown in Fig. 3(b), noise exacerbates the monotonic decay of decoherence.

As demonstrated in Fig. 3(c), when the ramp time scale decreases, indicating weaker coupling between the environment and the qubit, coherence increases and becomes less affected by noise. Furthermore, as shown in Fig. 3(b) and Fig. 3(c), the finite-size decoherence exhibits a sharp decay at the critical points $h_c = \pm 1$ for small ramp time scales, where the environment-qubit coupling is weak. In the case of strong coupling and large ramp time scales, the decay is observed specifically at $h_c = -1$. While for strong environment-qubit coupling, the decoherence exhibits a maximum at $h_c = 1$, as seen in Fig. 3(a). In other words, the critical points are signaled by the finite-size decoherence. In the absence of noise, the decoherence exhibits exponential scaling with the size of the system at the critical point, i.e.,

$$D|_{h=\pm 1} \sim e^{-N}.$$

In Fig. 4, we investigated the scaling behavior of the decoherence at the critical points in the presence of noise. We discovered that the decoherence exhibits exponential

scaling with $N\xi^2$, such that

$$D|_{h=\pm 1} \sim e^{-N\xi^2}.$$

B. Analysis in the presence of colored noise

The decoherence during a quench in the presence of colored (correlated) noise is plotted in Fig. 5 for different values of the ramp time scale. As seen in Fig. 5(a), when the environment-qubit coupling is strong enough, partial revivals are still present in the presence of colored noise, but they decrease as the noise correlation time τ_n decreases. This means that coherence is less affected by correlated noise than by white noise. Moreover, the period of the revivals remains the same in both noisy and noiseless cases. As shown in Fig. 5(b), in the case of weak coupling between the environment and the qubit, noise enhances the monotonic decay of decoherence. As the ramp time scale get smaller, which is equivalent to weaker environment-qubit coupling, the coherency increases and affected less by noise as illustrated in Fig. 5(c). Furthermore, it is clear that the critical points are signaled by the finite-size decoherence. In the presence of colored noise, we investigated the scaling behavior of the decoherence at the critical points. We found that the decoherence exhibits exponential scaling with $N\xi^2/\tau_n$, specifically,

$$D|_{h=\pm 1} \sim e^{-\frac{N\xi^2}{\tau_n}}.$$

In Appendix B more details are given on the scaling of D .

Fig. 6 illustrates the scaling of the revivals (the maximum of decoherence) in the presence of white and colored noise for $\tau_Q = 250$. As seen in Fig. 6(a), the maximum of the revivals scales exponentially with the square of the noise intensity. Additionally, the decreasing slope of the lines indicates the accumulation of noise-induced excitations during the evolution, which results in the decay of the revivals as the quench time t increases. The scaling of the revivals with the noise correlation time τ_n is depicted in

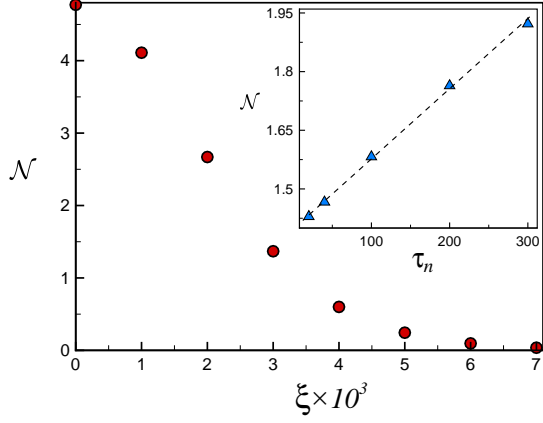


FIG. 7. The measure of non-Markovianity for the white, as a function of the noise strength and the inset shows the measure of non-Markovianity for the color noises versus the correlation time. In the inset panel the dashed black line is the best linear fit to the data. Here, we have $\xi = 0.003$.

Fig. 6(b) and Fig. 6(c) for the noise intensity $\xi = 0.003$. As observed, the maximum of the decoherence increases with the noise correlation time and scales linearly with τ_n for fast noise ($\tau_n \leq 100$), while it scales exponentially for slow noise ($\tau_n \geq 250$).

V. NON-MARKOVIANITY

The revivals in coherence of the central spin through the quench signals non-Markovianity of the dynamics. Here, to study the features of this behavior we quantify deviation of this dynamics from a Markovian one by computing the measure proposed in Ref. [51].

The measure is defined based on the rate of change in the trace distance between two initially distinguishable states $\rho_1(0)$ and $\rho_2(0)$ for a given process that we show as $\Phi(t)$. Indeed, for a Markovian process any two states become increasingly similar over time. Therefore, the measure is computed based on the deviation from this property as

$$\mathcal{N} = \int_{>0} dt \frac{d}{dt} \mathcal{D}[\Phi(t)\rho_1(0), \Phi(t)\rho_2(0)], \quad (19)$$

where the integration is only performed for the time intervals that the integrand is positive. Here,

$$\mathcal{D}[\rho_1, \rho_2] = \frac{1}{2} \|\rho_1 - \rho_2\|_1$$

is the trace distance with $\|\cdots\|_1$ standing for the trace norm [52]. The above quantity must be maximized for different initial states. For the pure dephasing of a central spin that we are interested in this work the superposition state already is the optimal state.

The results for the measure of non-Markovianity are shown in Fig. 7 for both white and colored noise cases.

In the case of white noise, we observe a monotonic decay in the non-Markovianity of the process as the noise strength increases. For large enough ξ values the process becomes fully Markovian. In order to understand the role of finite noise correlation time, we compute the measure in Eq. (19) with different τ_n values when the noise strength is fixed to $\xi = 0.003$. Interestingly, the measure exhibits a linear growth with the noise correlation time.

VI. SUMMARY AND CONCLUSION

Characterizing noisy signals is crucial for understanding the dynamics of open quantum systems, enhancing our ability to control and engineer them effectively. This work investigated the impact of noisy environmental spin systems (ESSs) on the decoherence of the central qubit as a sensitive noise estimator compared to other methods. We specifically focus on how noise in a time-dependent external magnetic field influences the coherence dynamics of a central spin coupled to a spin chain, particularly as the ESS is driven across its quantum critical point (QCP).

By extending the central spin model to incorporate stochastic variations in the external magnetic field, we demonstrate that noise not only amplifies decoherence resulting from the nonequilibrium critical dynamics of the environment but also profoundly affects the system's temporal evolution. Our numerical calculations reveal that decoherence exhibits exponential scaling at the critical points with both the square of the noise intensity and the noise correlation time. This contrasts with the noiseless case, where coherence revivals occur when the chain-qubit coupling is sufficiently strong; however, these revivals diminish in the presence of noise, scaling exponentially with white noise intensity and linearly or a power law in the case of colored noise, depending on the correlation time.

Additionally, our exploration of non-Markovianity reveals that it decreases with the square of the noise intensity but increases linearly with the noise correlation time, highlighting the complex interplay between noise and memory effects in quantum systems. These findings underscore the importance of accounting for noise to model and predict quantum system behavior under realistic conditions accurately. They also offer new perspectives on the challenges and opportunities in quantum control, decoherence mitigation, and potential applications in noise spectroscopy of external signals.

Last but not least, interference phenomena exemplified by the collapse and revival of the decoherence function serve as a direct evidence of entanglement dynamics and information flow between the central spin and the chain. But from a fundamental point of view the interference effect alone is not sufficient to rule out a classical description of the environment [53]; collapse and revival phenomena can indeed be generated by coupling the qubit to an engineered classical field [54]. Therefore, to

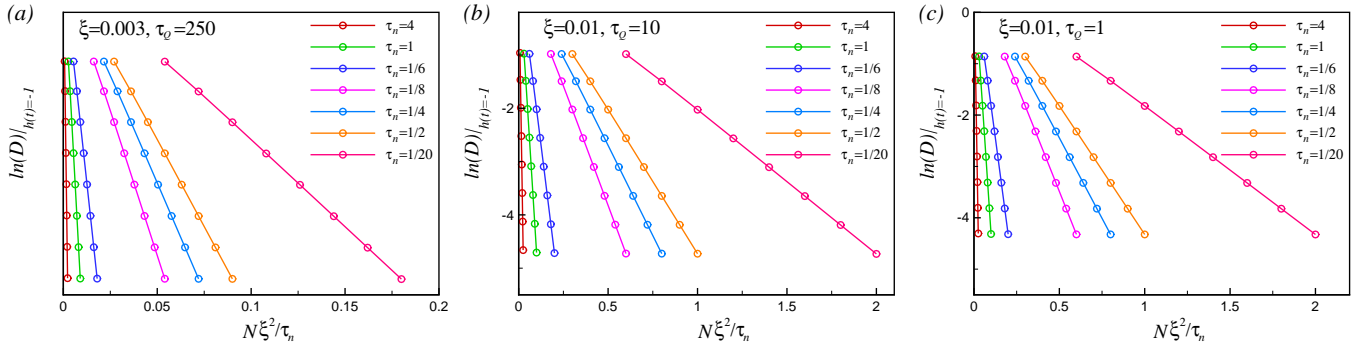


FIG. 8. Scaling of decoherence at the critical point $h_c = -1$ versus $N\xi^2/\tau_n$ for the ramp time scales: (a) $\tau_Q = 250$, $\xi = 0.003$, (b) $\tau_Q = 10$, $\xi = 0.01$, (c) $\tau_Q = 1$, $\xi = 0.01$.

definitively demonstrate the quantum nature of the system, a more fundamental approach is needed, similar to quantum-witness equality [55] and the Leggett-Garg test [54, 56]. Therefore, the present work anticipates a systematic exploration of entanglement dynamics and quantum coherence using stronger nonclassicality criterion for distinguishing quantum behavior from classical effects in various conditions.

ACKNOWLEDGEMENT

This work is based upon research funded by Iran National Science Foundation (INSF) under project No. 4024646.

Appendix A: Ensemble-averaged transition probabilities: Exact noise master equation

As shown in Refs. [42, 46], the noise-averaged density matrix $\rho_{st}(t)$ is described by the following nonperturbative exact master equation

$$\begin{aligned} \frac{d}{dt}\rho(t) = & -i[H_0(t), \rho(t)] \\ & -\frac{\xi^2}{2\tau_n} \left[H_1, \int_{t_i}^t e^{-\frac{|t-s|}{\tau_n}} [H_1(s), \rho(s)] ds \right]. \end{aligned} \quad (\text{A1})$$

The Hamiltonian of the transverse field Ising model can be written as a sum of decoupled k -mode Hamiltonians, and consequently, the density matrix of the model has a direct product structure $\rho(t) = \otimes_k \rho_k(t)$. Therefore, the noise master equation for the ensemble-averaged density matrix $\rho_k(t)$ takes the form

$$\begin{aligned} \frac{d}{dt}\rho_k(t) = & -i[H_{0,k}(t), \rho_k(t)] \\ & -\frac{\xi^2}{2\tau_n} \left[H_1, \int_{t_i}^t e^{-\frac{|t-s|}{\tau_n}} [H_1(s), \rho_k(s)] ds \right]. \end{aligned} \quad (\text{A2})$$

To solve for $\rho_k(t)$, we introduce a new operator defined by the integral in the same equation:

$$\Gamma_k(t) \equiv \int_{t_i}^t e^{-(t-s)/\tau_n} [H_1, \rho_k(s)] ds. \quad (\text{A3})$$

Equation (A1) then takes the form:

$$\dot{\rho}_k(t) = -i[H_k^{(0)}(t), \rho_k(t)] - \frac{\xi^2}{2\tau_n} [H_1, \Gamma_k(t)]. \quad (\text{A4})$$

By using the Leibniz integral rule, one obtains the derivative of $\Gamma_k(t)$ with respect to time as:

$$\dot{\Gamma}_k(t) = -\frac{\Gamma_k(t)}{\tau_n} + [H_1, \rho_k(t)]. \quad (\text{A5})$$

The elements of the ensemble-averaged density matrix $\rho_k(t)$ can now be obtained by numerically solving the coupled differential equations (A4) and (A5) with the initial conditions:

$$\rho_k(t_i) = \begin{pmatrix} 1 & 0 \\ 0 & 0 \end{pmatrix}, \quad \text{and} \quad \Gamma_k(t_i) = \begin{pmatrix} 0 & 0 \\ 0 & 0 \end{pmatrix}. \quad (\text{A6})$$

In the chosen basis, the first initial condition indicates that the system is initialized in the ground state, while the second condition signifies that the initial state is noiseless. Having obtained the ensemble-averaged density matrix $\rho_k(t)$ for a mode k from the master equation (A1), we can obtain the mean values of

$$\begin{aligned} |u_k^\pm(t)|^2 &= \rho_{k,(2,2)}(t), \\ |v_k^\pm(t)|^2 &= \rho_{k,(1,1)}(t), \\ u_k^\pm(t)v_k^{\pm*}(t) &= \rho_{k,(1,2)}(t), \\ u_k^{\pm*}(t)v_k^\pm(t) &= \rho_{k,(2,1)}(t). \end{aligned} \quad (\text{A7})$$

For comprehensive discussions and detailed expositions on the exact noise master equations, including the formal properties of the time-evolved averaged density matrix, we direct readers to Refs. [32, 46, 48–50].

Appendix B: Scaling of the decoherence factor at the critical points in the presence of colored noise

As noted in the main text, decoherence scales exponentially with $N\xi^2/\tau_n$, specifically:

$$D|_{h=\pm 1} \sim e^{-\frac{N\xi^2}{\tau_n}}.$$

This scaling behavior is depicted in Fig. 8, which shows how decoherence at the critical point $h_c = -1$ varies with $N\xi^2/\tau_n$ for different ramp time scales.

[1] A. Barenco and A. K. Ekert, *Journal of Modern Optics* **42**, 1253 (1995).

[2] S. F. Pereira, Z. Y. Ou, and H. J. Kimble, *Phys. Rev. A* **62**, 042311 (2000).

[3] A. Barenco, *Contemporary Physics* **37**, 375 (1996).

[4] L. K. Grover, *Phys. Rev. Lett.* **79**, 325 (1997).

[5] R. Jafari, *Phys. Rev. A* **82**, 052317 (2010).

[6] U. Mishra, H. Cheraghi, S. Mahdavifar, R. Jafari, and A. Akbari, *Phys. Rev. A* **98**, 052338 (2018).

[7] A. Einstein, B. Podolsky, and N. Rosen, *Phys. Rev.* **47**, 777 (1935).

[8] J. S. Bell, *Physics* **1**, 195 (1964).

[9] W. H. Zurek, *Rev. Mod. Phys.* **75**, 715 (2003).

[10] J. P. Paz. and W. H. Zurek, in *coherent matter waves* (EDP Sciences, Springer Ver- lag, Berlin, 2001) pp. 533–614.

[11] R. Jafari and H. Johannesson, *Phys. Rev. Lett.* **118**, 015701 (2017).

[12] R. Jafari and H. Johannesson, *Phys. Rev. B* **96**, 224302 (2017).

[13] R. Jafari and A. Akbari, *EPL (Europhysics Letters)* **111**, 10007 (2015).

[14] S. Sachdev, *Handbook of Magnetism and Advanced Magnetic Materials* (2007).

[15] J. Schliemann, A. V. Khaetskii, and D. Loss, *Phys. Rev. B* **66**, 245303 (2002).

[16] F. M. Cucchietti, J. P. Paz, and W. H. Zurek, *Phys. Rev. A* **72**, 052113 (2005).

[17] M. Kiciński and J. K. Korbicz, *Phys. Rev. A* **104**, 042216 (2021).

[18] F. M. Cucchietti, C. H. Lewenkopf, and H. M. Pastawski, *Phys. Rev. E* **74**, 026207 (2006).

[19] S. Suzuki, T. Nag, and A. Dutta, *Phys. Rev. A* **93**, 012112 (2016).

[20] T. Nag, U. Divakaran, and A. Dutta, *Phys. Rev. B* **86**, 020401 (2012).

[21] H. T. Quan, Z. Song, X. F. Liu, P. Zanardi, and C. P. Sun, *Phys. Rev. Lett.* **96**, 140604 (2006).

[22] T. Kibble, *Physics Today* **60**, 47 (2007).

[23] W. H. Zurek, *Nature* **317**, 505 (1985).

[24] H. Pichler, J. Schachenmayer, J. Simon, P. Zoller, and A. J. Daley, *Phys. Rev. A* **86**, 051605 (2012).

[25] X. Chen, A. Ruschhaupt, S. Schmidt, A. del Campo, D. Guéry-Odelin, and J. G. Muga, *Phys. Rev. Lett.* **104**, 063002 (2010).

[26] P. Zoller, G. Alber, and R. Salvador, *Phys. Rev. A* **24**, 398 (1981).

[27] P. Doria, T. Calarco, and S. Montangero, *Phys. Rev. Lett.* **106**, 190501 (2011).

[28] J. Marino and A. Silva, *Phys. Rev. B* **86**, 060408 (2012).

[29] J. Marino and A. Silva, *Phys. Rev. B* **89**, 024303 (2014).

[30] A. Dutta, A. Rahmani, and A. del Campo, *Phys. Rev. Lett.* **117**, 080402 (2016).

[31] Y. Bando, Y. Susa, H. Oshiyama, N. Shibata, M. Ohzeki, F. J. Gómez-Ruiz, D. A. Lidar, S. Suzuki, A. del Campo, and H. Nishimori, *Phys. Rev. Res.* **2**, 033369 (2020).

[32] A. Chenu, M. Beau, J. Cao, and A. del Campo, *Phys. Rev. Lett.* **118**, 140403 (2017).

[33] M. Abdi, S. Barzanjeh, P. Tombesi, and D. Vitali, *Phys. Rev. A* **84**, 032325 (2011).

[34] P. Pfeuty, *Ann. Phys.* **57**, 79 (1970).

[35] B. Damski, H. T. Quan, and W. H. Zurek, *Phys. Rev. A* **83**, 062104 (2011).

[36] Z. Sun, X. Wang, and C. P. Sun, *Phys. Rev. A* **75**, 062312 (2007).

[37] Z. Sun, J. Ma, X.-M. Lu, and X. Wang, *Phys. Rev. A* **82**, 022306 (2010).

[38] T. A. Costi and R. H. McKenzie, *Phys. Rev. A* **68**, 034301 (2003).

[39] E. Lieb, T. Schultz, and D. Mattis, *Annals of Physics* **16**, 407 (1961).

[40] R. Jafari, *The European Physical Journal B* **85**, 167 (2012).

[41] B. Damski, *Phys. Rev. Lett.* **95**, 035701 (2005).

[42] R. Jafari, A. Langari, S. Eggert, and H. Johannesson, *Phys. Rev. B* **109**, L180303 (2024).

[43] S. Zamani, J. Naji, R. Jafari, and A. Langari, *Journal of Physics: Condensed Matter* **36**, 355401 (2024).

[44] R. Baghram, R. Jafari, and A. Langari, *Phys. Rev. B* **110**, 064302 (2024).

[45] A. A. Budini, *Physical Review A* **64**, 052110 (2001).

[46] A. Kiely, *EPL* **134**, 10001 (2021).

[47] S. Sharma, U. Divakaran, A. Polkovnikov, and A. Dutta, *Phys. Rev. B* **93**, 144306 (2016).

[48] J. Luczka, *Czechoslov. J. Phys.* **41**, 289 (1991).

[49] A. A. Budini, *Phys. Rev. A* **63**, 012106 (2000).

[50] J. I. Costa-Filho, R. B. B. Lima, R. R. Paiva, P. M. Soares, W. A. M. Morgado, R. L. Franco, and D. O. Soares-Pinto, *Phys. Rev. A* **95**, 052126 (2017).

[51] H.-P. Breuer, E.-M. Laine, and J. Piilo, *Phys. Rev. Lett.* **103**, 210401 (2009).

[52] M. A. Nielsen and I. L. Chuang, *Quantum Computation and Quantum Information: 10th Anniversary Edition* (Cambridge University Press, 2011).

- [53] A. J. Leggett, *Journal of Physics: Condensed Matter* **14**, R415 (2002).
- [54] A. J. Leggett and A. Garg, *Phys. Rev. Lett.* **54**, 857 (1985).
- [55] C.-M. Li, N. Lambert, Y.-N. Chen, G.-Y. Chen, and F. Nori, *Scientific reports* **2**, 885 (2012).
- [56] A. Asadian, C. Brukner, and P. Rabl, *Phys. Rev. Lett.* **112**, 190402 (2014).